Heliyon 10 (2024) e35235

Contents lists available at ScienceDirect

Heliyon

journal homepage: www.cell.com/heliyon

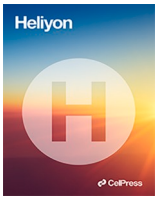

Research article

# The identification of heterogeneous reactive oxygen subtypes in esophageal squamous cell carcinoma to aid patient prognosis and immunotherapy

Qiang Lu [a,1], Qi Yang [b,1], Jinbo Zhao [a,1], Guizhen Li [a], JiPeng Zhang [a], Chenghui Jia [a], Yi Wan [c,*], Yan Chen [d,**]

[a] Department of Thoracic Surgery, Tangdu Hospital, Air Force Medical University, 569 Xinsi Road, Xi'an, 710038, China
[b] Precision Pharmacy & Drug Development Center, Department of Pharmacy, Tangdu Hospital, Fourth Military Medical University, Xi'an, 710038, China
[c] Department of Health Service, Air Force Medical University, No.169 Changle West Road, Xi'an, 710032, China
[d] Department of Oncology, Xijing Hospital, Air Force Medical University, No. 169 Changle West Road, Xi'an, 710032, China

ARTICLE INFO

*Keywords:*
Esophageal squamous cell carcinoma (ESCC)
Reactive oxygen species (ROS)
Subtypes
Immune infiltration
Immunotherapy

ABSTRACT

*Introduction:* Esophageal cancer is increasingly recognized as a significant global malignancy. The main pathological subtype of this cancer is esophageal squamous cell carcinoma (ESCC), which displays a higher degree of malignancy and a poorer prognosis. Reactive oxygen species (ROS) play a critical role in modulating the immune response to tumors, and understanding the regulation of ROS in ESCC could lead to novel and improved therapeutic strategies for ESCC patients.
*Methods:* A consensus matrix derived from genes involved in the ROS pathway revealed two subtypes of ROS. These subtypes were categorized as ROS-active or ROS-suppressive based on their level of ROS activity. The heterogeneity among the different ROS subtypes was then explored from various perspectives, including gene function, immune response, genomic stability, and immunotherapy. In order to assess the prognosis and the potential benefits of immunotherapy, a ROS activity score (RAS) was developed using the identified ROS subtypes. In vitro experiments were performed to confirm the impact of core RAS genes on the proliferative activity of esophageal cancer cell lines.
*Results:* Two distinctive subtypes of ROS were identified. The first subtype, referred to as ROS-active, exhibited elevated ROS activity, enhanced involvement in cancer-associated immune pathways, and increased infiltration of effector immune cells. The second subtype, named ROS-suppressive, demonstrated weaker ROS activity but displayed more pronounced dysregulation in the cell cycle and a denser extracellular matrix, indicating malignant characteristics. Genomic stability, particularly in terms of copy number variation (CNV) events, differed between the two ROS subtypes. By developing a RAS model, reliable risk assessment for overall survival (OS) in patients with ESCC was achieved, and the model demonstrated strong predictive capabilities in real-world immunotherapy cohorts. Moreover, the core gene LDLRAD1 within the RAS model was found to enhance proliferative activity in esophageal cancer cell lines.

* Corresponding author.
** Corresponding author.
*E-mail addresses:* wanyi@fmmu.edu.cn (Y. Wan), chenyanfmmu@163.com (Y. Chen).
[1] Co-first authors: Qiang Lu, Qi Yang, and Jinbo Zhao.

https://doi.org/10.1016/j.heliyon.2024.e35235
Received 20 January 2024; Received in revised form 24 July 2024; Accepted 24 July 2024
Available online 29 July 2024

*Conclusion:* Based on the ROS pathway, we successfully identified two distinct subtypes in ESCC: the ROS-active subtype and the ROS-suppressive subtype. These subtypes were utilized to evaluate prognosis and the sensitivity to immunotherapy.

## 1. Introduction

Esophageal cancer is one of the prevalent malignancies in the digestive system. Recent statistics show that the incidence of esophageal cancer has risen to the seventh highest rate globally [1]. In China, the majority of esophageal cancer patients (about 90 %) have the histological subtype of esophageal squamous cell carcinoma (ESCC) [2]. ESCC has a high degree of malignancy and poor prognosis, with a 5-year overall survival rate of less than 20 % for advanced ESCC [3,4]. For patients with unresectable advanced ESCC, chemotherapy and radiotherapy are the main treatment options [5]. In recent years, immunotherapy has emerged as a very promising direction in cancer treatment, showing surprising therapeutic effects in a variety of solid tumors (e.g., non-small cell lung cancer, melanoma) [6,7]. We can expect to combine the development of immunotherapy with conventional treatments to improve the clinical outcome of ESCC patients [5]. Regrettably, because of the variability in treatment response across patients, novel biomarkers are needed to assist in risk stratification and to determine the optimal immunotherapy protocols.

Reactive oxygen species (ROS) refer to a class of highly reactive chemicals derived from oxygen molecules, including superoxide ions, hydroxyl radicals, and hydrogen peroxide [8]. Reactive oxygen species (ROS) have complex and multiple roles in cancer. On the one hand, ROS can induce DNA damage and apoptosis, which help to inhibit tumor proliferation and expansion [9]. On the other hand, ROS can also promote tumor development by stimulating cell proliferation and angiogenesis [6]. Recent findings also suggest that different ROS levels can influence the immune response to cancer cells, thus affecting antitumor immune activity and immunotherapeutic efficacy [10,11]. Dendritic cells and T cells act as effector cells of antitumor immunity, infiltrating into specific sites through antigen stimulation in the tumor microenvironment, thereby exerting antitumor effects [12,13]. The excessive amount of ROS can act as a stimulatory source for the immune system to generate potential antigen stimulation to enhance this convening process [14]. In addition, specific concentrations of ROS levels can inhibit the activity of tumor cells in secreting suppressive cytokines as well as reduce the infiltration and activity of suppressive immune cells, ultimately leading to a reduction in immune escape and thus enhancing the tumor response to immunotherapy [10,15]. Therefore, it is a challenging question to regulate the appropriate ROS levels in cancer therapy to take advantage of the anti-tumor effects promoted by ROS. However, the mechanisms by which ROS levels promote effective tumor treatment remain elusive. Studying ROS regulation in ESCC is expected to be a promising direction for improving the clinical management of patients.

In this study, we focused on the potential crosstalk of ROS-related genes (RRGs) in ESCC. We identified and confirmed two heterogeneous subtypes (ROS-active and ROS-suppressive) in ESCC based on RRGs. They were heterogeneous in immune activity, biological function, genomic stability, and immunotherapeutic response. Based on these two heterogeneous ROS subtypes we developed a validated tool to assess ROS levels, called Ros active score (RAS), which can effectively predict the prognosis of ESCC patients and evaluate the effect of immunotherapy.

## 2. Methods

### 2.1. Data acquisition and preprocessing

We obtained transcriptomic RNA-seq data, genomic mutation data based on Muctect 2 platforms, and copy number variation (CNV) profiles processed by gistic2.0 for the TCGA-ESCA cohort in the UCSC Xena database (https://xena.ucsc.edu/) and collected corresponding clinical follow-up information. We screened out patients with clear pathological subtypes of ESCC and excluded those with incomplete follow-up information, and finally obtained a TCGA-ESCC cohort containing 80 ESCC patients as a training cohort. The Count matrix of the raw RNA-Seq data was normalized to obtain the Transcripts Per Kilobase Million (TPM) matrix. In addition, a large-scale ESCC cohort (GSE53625) was selected from the GEO database for external validation, and a total of 179 patients with esophageal cancer were included for use as the GEO-ESCC cohort and analyzed after excluding patients with incomplete follow-up information. Patient follow-up information was obtained from the original supplemental material. The raw RNA-Seq data were log2-processed. Data for the TCGA pan-cancer cohort were also collected from the UCSC Xena database, and the integrated TPM sequencing matrix as well as the response clinical information were downloaded.

### 2.2. Consensus clustering to identify heterogeneous ROS subgroups

The ROS-related genes (RRGs) were collected from the GO-biological process gene set of the MSigDB database (http://www.gsea-msigdb.org/gsea/index.jsp) [16]. A total of 1426 RRGs were included, and the detailed gene list has been uploaded as Table S1. First, RRGs with independent predictive effects on the overall survival (OS) of ESCC patients were recognized by one-way Cox regression analysis. Subsequently, candidate RRGs were collected based on a threshold of $P < 0.05$ and input into the consensus clustering pipeline. Consensus clustering based on the transcriptional profiles of candidate RRGs using the "ConsensusClusterPlus" software package has been applied to identify isoforms with different ROS heterogeneity [17]. The analysis performs clustering in discovery and validation cohorts with a core Pam unsupervised clustering algorithm that assesses the neighborhood of samples based on Spearman

correlation. Randomly selected 80 % of the samples were subjected to 1000 iterations to finally determine the best consensus matrix with clustering numbers of 2–5, respectively. The spearman adjacency consensus matrix and cumulative distribution function (CDF) were jointly used to determine the optimal number of clusters to generate ROS subtypes.

### 2.3. Dissecting biological function and immune heterogeneity

We used the "limma" algorithm to identify differentially expressed genes (DEGs) of different ROS subtypes. Significant DEGs were identified based on the Fold change>2 and adjusted P-value <0.05 threshold. DEGs were uploaded to the Metascape (www.metascape.org/) online platform for functional annotation. We then conducted GSEA analysis to assess relative activity of the KEGG pathway gene set across different ROS subtypes utilizing GSEA software (Version 4.1.0), and significantly enriched KEGG pathways were identified based on a $P < 0.05$ threshold.

To assess the immune heterogeneity of different ROS subtypes, we first assessed the relative immune activity scores of individual samples based on immune and matrix markers by the "ESTIMATE" algorithm [18]. Subsequently, the distribution of typical immune checkpoints was examined for differences between subtypes. We also assessed the relative infiltration abundance of 22 different immune cells based on their transcriptional characteristics by the "CIBERSORT" algorithm [19]. We also assessed the relative activity of immune-related pathways of interest based on published gene sets by the ssGSEA algorithm. Finally, we convened Homologous Recombination Deficiency (HRD), microsatellite instability (MSI) score, and SNV neoantigens in TCGA-ESCC patients from the previous literature [20].

### 2.4. Dissecting the heterogeneity of genomic stability

We used the "maftools" R package for Maf file processing and visualization of somatic mutations [21]. After excluding nonsignificant mutant fragments, we counted the total mutation burdens (TMB) of individual patients and collected genes with minimum mutation number >5 for analysis. Then, the differences in mutation frequencies of high-frequency mutated genes between the two subgroups were compared using chi-square tests and visualized using forestplot. After merging all the mutation information to be presented, the mutation maps of different ROS subtypes were drawn using maftools. When processing CNV data, we used Gistic 2.0 software and set a threshold of 0.2. With this threshold, we identified significantly amplified and missing chromosomal segments and assessed CNV differences on chromosomal arms. Finally, we visualized the CNV status by the R package ggpubr. In this way, we were able to compare the CNV profiles of different subgroups more visually.

### 2.5. Construction of ROS activity scores

We selected the previous-identified ROS-related DEGs between the two ROS subtypes that were common to all cohorts for further analysis by integrating the results of univariate Cox regression and log-rank tests to reveal the prognostic value of DEGs for OS. DEGs with statistical significance were entered into the ROS activity score generation pipeline. Specifically, we used iterative LASSO regression to retrieve the most stable predictive model. A 5-fold cross-validation and "maxit = 1000″ were set to prevent model overfitting. Using the minimum lambda value as a penalty factor and generating risk coefficients for the model genes, ROS activity scores (RAS) were generated according to the following formula:

$$RAS = \sum iCoefficient(mRNA_i) \times Expression(mRNA_i)$$

The median RAS-based score was used to distinguish between high-risk and low-risk ESCC patients. The C-index was generated from the "pec" package to assess the predictive power of the RAS, with a higher C-index indicating better prediction [22]. The prognostic efficacy of RAS was then evaluated by KM survival curves, univariate and multifactorial Cox regression, ROC curves, and COX subgroup regression analysis.

### 2.6. Assessment of ROS-related immunotherapy response

To exam the benefit rates of ESCC patients to respond to immunotherapy, we calculated the Immunophenoscore (IPS) of individual patients by analyzing the number and type of immune-related cells in the patients' tumor tissues [23]. Higher IPS values indicate that the patients' immune system is more capable of attacking the tumor and therefore may respond better to immunotherapy. In addition, we used the TIDE algorithm (http://tide.dfci.harvard.edu) to predict response rates to anti-PD-1 and anti-CTLA-4 treatments of ESCC patients by assessing the interaction between tumor cells and immune cells and the degree of T-cell exhaustion [24–27]. Finally, we generated RAS by the same formula in two established immunotherapy cohorts (Imvigor210 and nature-SKCM) to validate the predictive effect of immunotherapy [28,29].

### 2.7. Cell culture and transfection

We purchased two esophageal cancer cell lines (ECA-109 and TE1) from EK-bioscience (China) and cultured them in DMEM medium (Bological, Israel) supplemented with 10 % heat-inactivated FBS, 1 % penicillin and streptomycin, placed in a constant temperature 37 °C incubator containing 5 % $CO_2$. Lipofectamine 8000 reagent (Invitrogen, USA) was used to transiently transfect

siRNA to silence the expression of specific genes according to the manufacturer's instructions. We used the following siRNAs and their blank transfer controls: si-LDLRAD1: AGAGAATGGCTACACTGCTGCTGAA; siNC: AGAGTATCGACAGTCGTCTCGAGAA.

### 2.8. Cell counting Kit-8 assay

The proliferation viability of ESCC cells was measured using Cell Counting Kit-8 (CCK-8, Bioss, China) according to the instructions of the kit. The absorbance at 450 nm was measured using an enzyme-linked immunoassay (BioTek, USA) for cell growth until 12 h, 24 h, 36 h, 48 h and 72 h, respectively.

### 2.9. Pan-cancer analysis

Using data from the TCGA pan-cancer cohort, we performed a systematic analysis of the RAS. We analyzed the mutations of ROS genes in the pan-cancer cohort using the maftools package. We analyzed the prognostic efficacy of RAS in the pan-cancer cohort by one-way Cox regression and log-rank test. Finally, we evaluated RAS-related biological pathways using the ssGSEA algorithm.

### 2.10. Statistical analysis

The *t*-test or Wilcoxon rank test was selected appropriately according to the characteristics of the variables to compare continuous variables between two groups, and the KM survival curves were plotted using the "survminer" packages. We then used the R packages "rms" and "survival" to perform univariate and multivariate cox regression analysis and to complete the nomogram visualization, and the R package "survROC" was used to implement the time-dependent ROC (tROC) analysis. Two-tailed $p < 0.05$ was considered statistically significant if not otherwise specified.

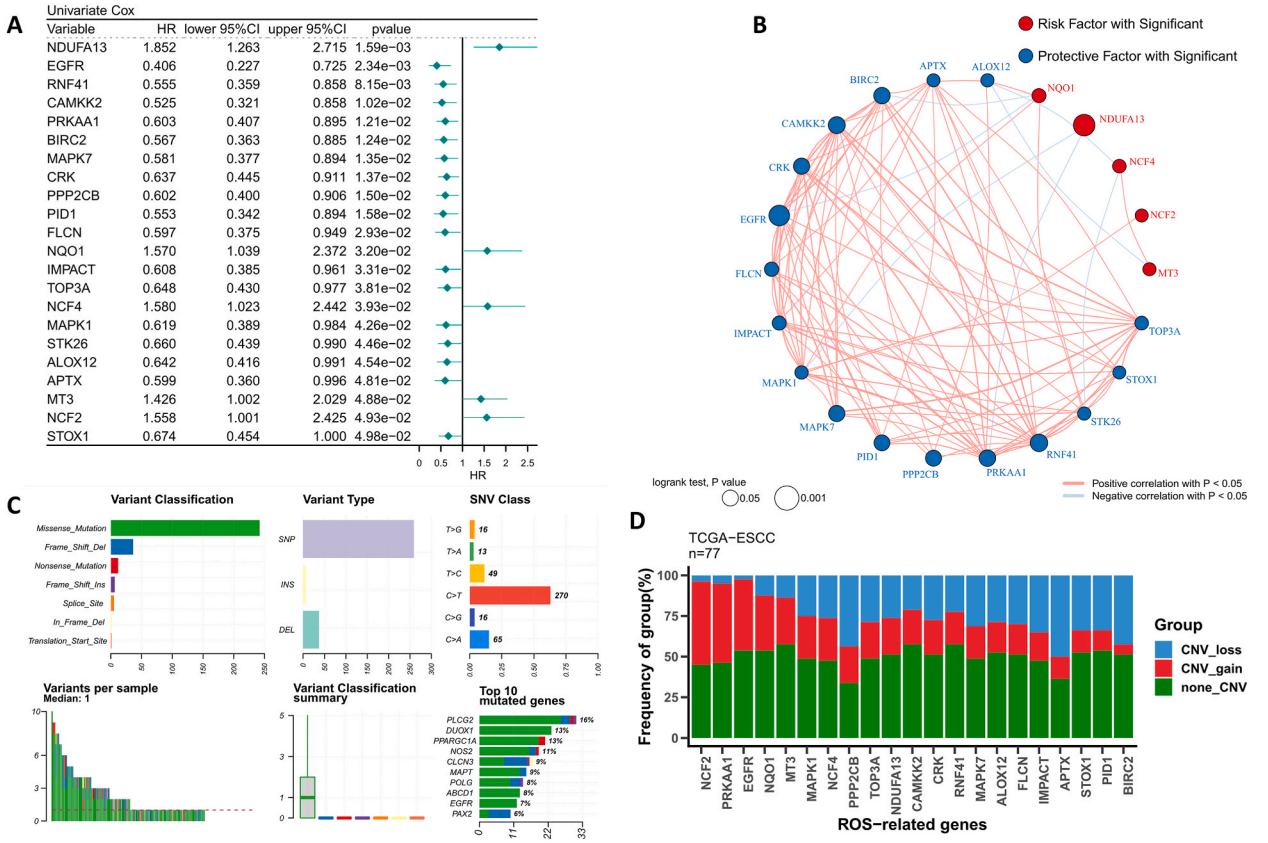


**Fig. 1.** Identification of ROS-related genes in TCGA-ESCA (A) Univariate Cox regression identified 22 ROS-related genes with prognostic efficacy. (B) The correlation network of 22 ROS-related genes. (C) The summary of somatic mutation of 22 ROS-related genes. (D) The summary of CNV status of 22 ROS-related genes.

## 3. Results

### 3.1. Dissecting ROS-related genes in TCGA-ESCC

We first performed univariate Cox regression to identify the 1426 RRGs with independent prognostic efficacy, and finally identified 22 prognostic RRGs based on a threshold of $P < 0.05$ (Fig. 1A). We mapped the interaction network of these 22 prognostic RRGs (Fig. 1B), and we found that most of the RRGs had significant and strong positive correlations. Except for NDUFA13, there were significant negative correlations between this gene and 4 other RRGs (ALOX12, MAPK1, PRKAA1 and STK26) (Fig. 1B). We summarized the single nucleotide mutation events of these 22 RRGs (Fig. 1C). Most of the mutations were missense mutations, with the most frequently mutated site was cytosine to thymine. The three genes with the highest mutation frequency (14 %) were PID1, EGFR and CAMKK2. Finally, we summarized the CNV profiles of 22 prognostic RRGs in ESCC, which showed that NCF2, PRKAA1 and EGFR were the most frequently amplified genes, while APTX, PPP2CB were the most frequently missing genes (Fig. 1D). Notably, APTX and PPP2CB were also the genes with the highest total CNV frequencies.

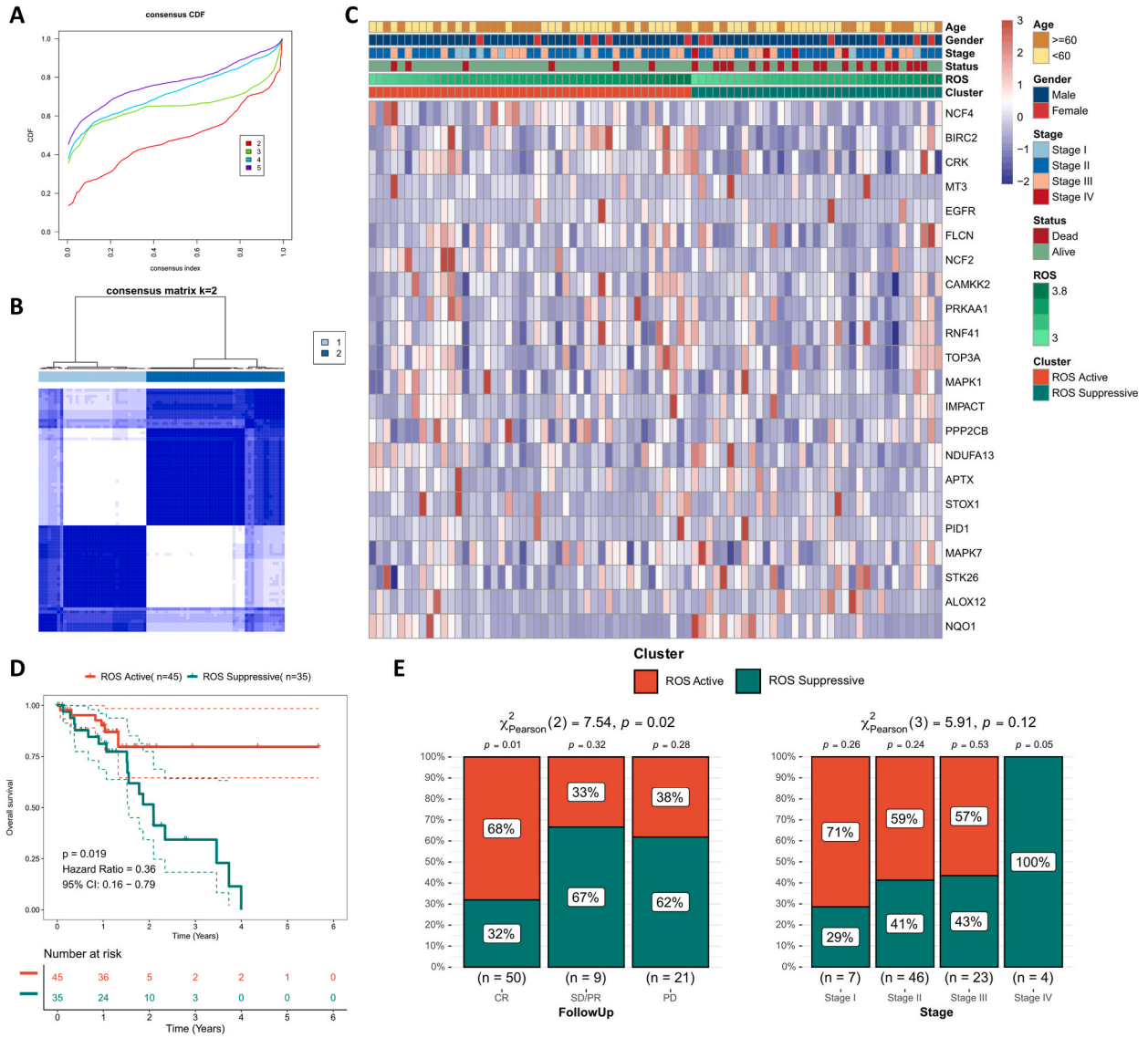


**Fig. 2.** Identification of heterogeneous ROS subtypes in TCGA-ESCA (A) The CDF curves of ROS consensus matrix. (B) The adjacency consensus matrix of ROS genes when K = 2. (C) Heat map showing clinical features and transcriptional profiles of ROS genes in two ROS subtypes. (D) KM survival curves of different ROS subtypes. (E) Differences in clinical outcomes (left) and stage (right) of ESCC patients with different ROS subtypes.

### 3.2. Identification of heterogeneous ROS subtypes

We first performed consensus clustering on the discovery cohort from TCGA-ESCC and GEO-ESCC cohort respectively and generated a consensus matrix using 22 prognostic RRGs. Based on the CDF curve of the consensus score and the adjacency of the consensus matrix, k = 2 is suitable as an appropriate number of clusters (Fig. 2A and B, Figs. S1A–B). Fig. 2C showed the different ROS activity in two clusters, after assessing the ROS pathway activity and expression of RRGs in the subtypes, we defined ROS-active subtypes with more ROS activity and ROS-suppressed subtypes with less ROS activity (Fig. 2C, Fig. S1C). Survival analysis revealed that the ROS-active subtype was found to have significantly better survival than the ROS-suppressed subtype in the TCGA-ESCC cohort (P = 0.019, Fig. 2D). A worse clinical outcome for the ROS-suppressed subtype was confirmed in the external validation ESCC cohort (P = 0.046, Fig. S1D). Moreover, a significantly higher proportion of patients with ROS-active subtypes and a lower proportion with stable disease and disease progression were observed in the TCGA-ESCC cohort. Patients with earlier-staged ESCC were more numerous in the ROS-active subtype, and notably, all patients in stage IV were in the ROS-suppressed subtype (Fig. 2E). Due to the lack of data in the GEO-ESCC cohort, more patients with stage I were observed only in the ROS-active subtype, while more patients with stage II and III ESCC were in the ROS-suppressed subtype (Fig. S1E).

### 3.3. Biological functional heterogeneity of different ROS subtypes

We first identified 629 significant ROS-related DEGs by limma package, of which 136 DEGs were up-regulated in ROS-active subtype and 493 DEGs were up-regulated in ROS-suppressive subtype. Functional enrichment analysis showed that upregulated DEGs in ROS-active subtypes were mainly involved in the innate immune response, digestion, and extracellular matrix (Fig. 3A). GSEA analysis revealed that the KEGG pathways enriched in the ROS-active subtype were mainly antigen processing and presentation, chemokine signaling pathway, cytokine receptor and NK cell-mediated cell killing (Fig. 3C). While in ROS suppressive subtype, the pathways enriched in the ROS inhibitory subtype were peroxisome, spliceosome, and aminoacyl trna biosynthesis (Fig. 3B–D). In conclusion, these results suggest that the ROS-active subtype has stronger antitumor immune activity, while the ROS-suppressed subtype has stronger cell cycle dysregulation and proliferative activity in tumor cells, which may ultimately guide the difference in survival of ESCC patients in different ROS subgroups.

### 3.4. Immunological heterogeneity of different ROS subtypes

We then systematically analyzed the immunological heterogeneity of the two ROS subtypes from several perspectives. First, the ESTIMATE algorithm showed that immune scores and Estimate scores were increased in the ROS-active subtype, while the ROS-suppressed subtype had higher tumor purity (Fig. 4A), we also found similar results in the GEO-ESCC cohort (Fig. S2A). We then examined the transcriptome expression differences of six classical immune checkpoints and therapeutic targets (CTLA-4, LAG-3, TIM-3, PD-1, PD-L1, and PD-L2), and found that all six immune genes were significantly upregulated in the ROS-active subtype (Fig. 4B), and this finding was confirmed in the validation cohort (Fig. S2B). Subsequently, the pathway activity of interest was assessed by the

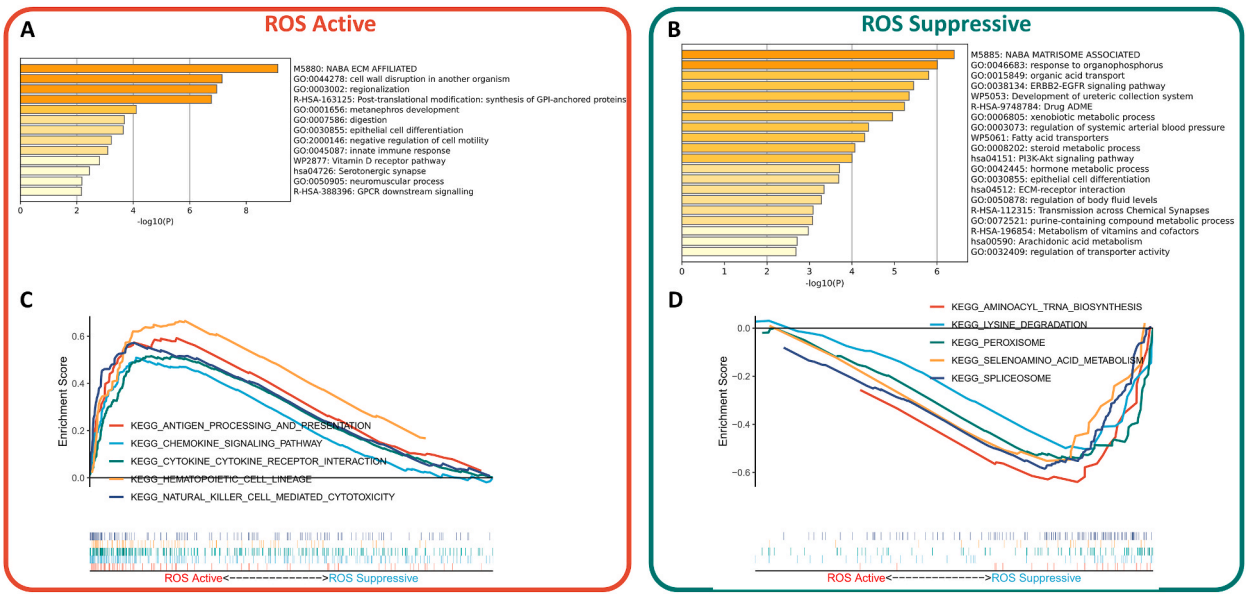


**Fig. 3.** Heterogeneity of biological functions in different ROS subtypes (A) Functional enrichment of genes characteristic of ROS-active subtypes. (B) Functional enrichment of genes characteristic of ROS-suppressive subtypes. (C) The top five KEGG pathways enriched in ROS-active subtypes. (D) Top five KEGG pathways enriched in ROS-suppressive subtypes.

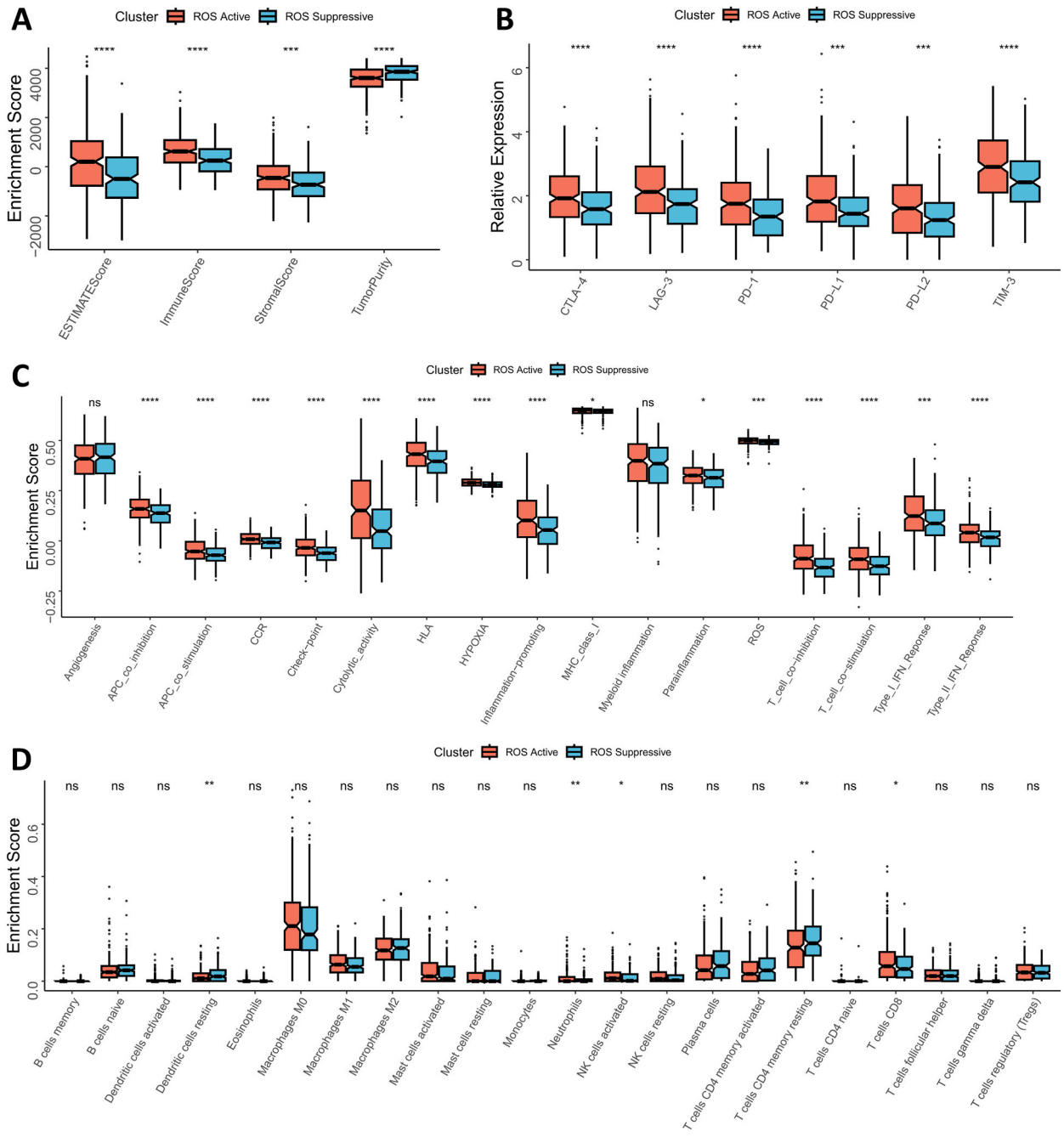


**Fig. 4.** Heterogeneity of immune activity in different ROS subtypes (A) Differences in Estimate scores between different ROS subtypes. (B) Differences in the expression of six typical immune checkpoints (CTLA-4, LAG-3, TIM-3, PD-1, PD-L1, and PD-L2) among different ROS subtypes. (C) Differences in anti-tumor immune-related pathway activities among different ROS subtypes. (D) Differences in the relative infiltration abundance of 22 immune cell types among different ROS subtypes. *: $P < 0.05$, **: $P < 0.01$, ***: $P < 0.001$, ****: $P < 0.0001$, ns: not significant.

ssGSEA algorithm, and the ROS active subtype had significantly elevated ROS pathway activity and hypoxic activity (Fig. 4C). In addition, immune-related pathways except myeloid immunity were upregulated in the ROS active subset (Fig. 4C). The GEO-ESCC cohort had similar results, and notably, the APC co-inhibitory pathway was upregulated in the ROS suppressive subtype in the validation cohort (Fig. S2C). Finally, the relative infiltration of immune cells was identified by CIBERSORT, and we found that in the TCGA-ESCC cohort, ROS-active subtypes of resting dendritic cells and CD4 T cells were decreased, whereas neutrophils, activated NK cells, and CD8 T cells were increased (Fig. 4D). In contrast, in the GEO-ESCC cohort, not only similar results were observed, but also most immune cells were found to be rising in the ROS-activated subset (Fig. S2D).

### 3.5. Genomic stability heterogeneity of different ROS subtypes

Firstly, the tumor mutational burdens (TMB) after excluding nonsignificant mutated fragments were counted by maftools, and we found no significant difference in TMB between ROS-active and ROS-suppressed subtypes (Fig. 5A). A chi-square test was performed to determine whether high-frequency mutated (mutation number >5) genes were different between subgroups, and the results showed that the mutation frequency of TRRAP was significantly higher in the ROS-active subtype (Fig. 5B). After summarizing all the mutation information, the mutation profile of high-frequency mutated genes among subtypes was mapped by oncoplot (Fig. 5C). CNV occurring on chromosomal segments is another form of mutation in the genome, and we further evaluated the correlation between ROS subtypes

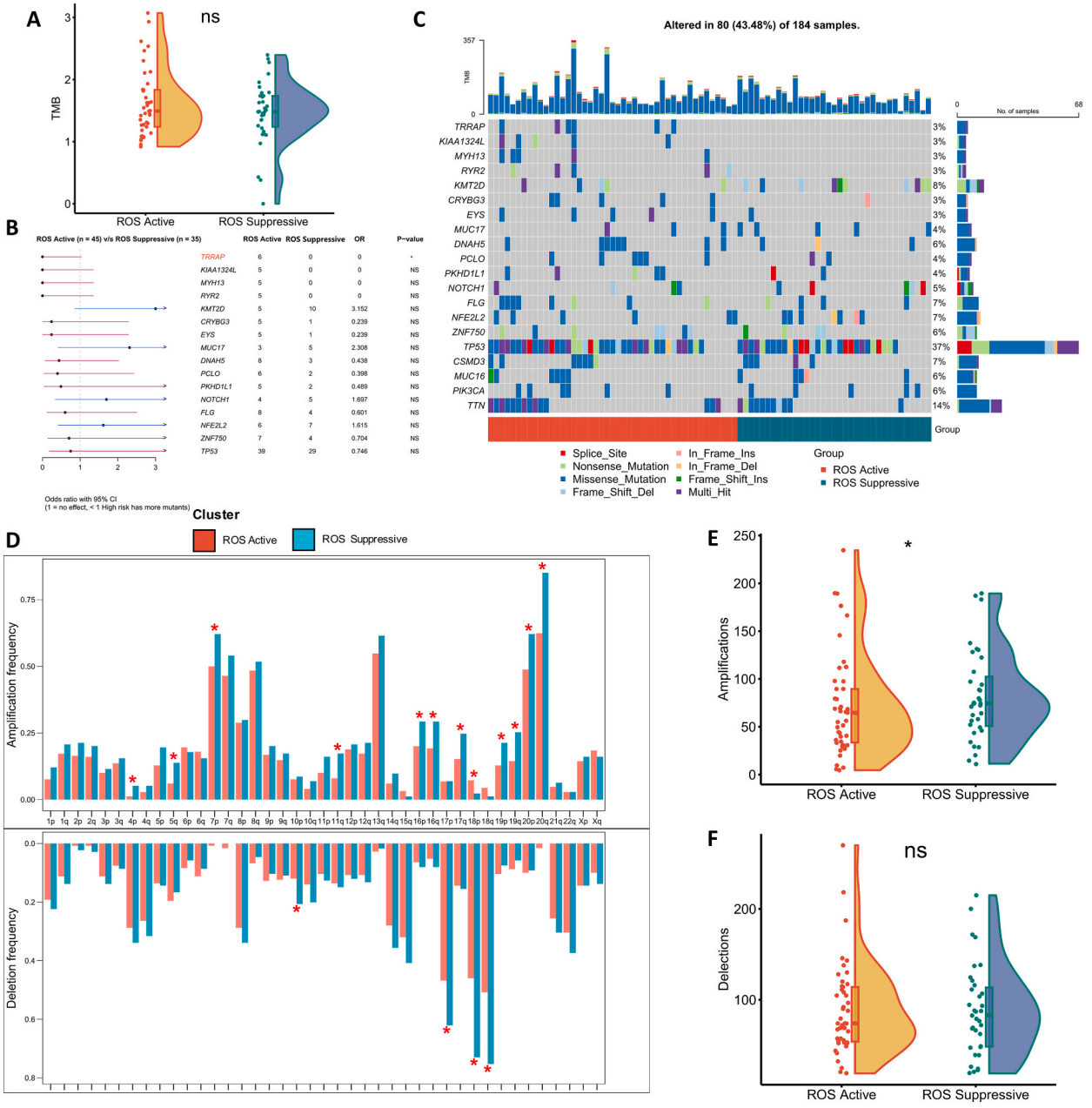


**Fig. 5.** Heterogeneity of genomic stability in different ROS subtypes (A) Differences in TMB among different ROS subtypes. (B) Forest plot showing the difference in frequency of significantly mutated genes among different ROS subtypes. (C) oncoplot showing the mutation profile of high-frequency mutated genes among ROS subtypes after summarizing the mutation information. (D) Histogram resolving CNV events on each chromosome arm among different ROS subtypes. (E) Differences in overall amplification numbers among different ROS subtypes. (F) Differences in the overall number of deletions between different ROS subtypes. *: $P < 0.05$, ns: not significant.

and CNV. We found significantly higher levels of amplification and deletion of ROS suppressor isoforms at the chromosome arm level (Fig. 5D). Total CNV events were counted for individual samples, and we found that patients with ROS suppressor subtypes had higher amplification counts (Fig. 5E), while deletion counts did not differ significantly between the two subtypes (Fig. 5F).

### 3.6. Immunotherapy heterogeneity across ROS subtypes

We first assessed the relationship between three immunotherapy-related indicators (HRD, MSI, and SNV neoantigens) and ROS subtypes. We found no significant difference in HRD between ROS subtypes (Fig. 6A). In contrast, ROS active subtypes had significantly higher MSI and SNV neoantigens (Fig. 6B and C). In the TCGA-ESCC cohort, we found higher IPS in the ROS active subtype (Fig. 6D). As assessed by the TIDE algorithm, we found significantly more patients in the ROS-active subtype who may be responsive to immunotherapy (Fig. 6E). In the GEO-ESCC cohort, we did not find significant differences in IPS between ROS subtypes (Fig. 6F). However, the TIDE results suggest that the ROS-active subtype in the GEO-ESCC cohort also has more patients who may benefit from

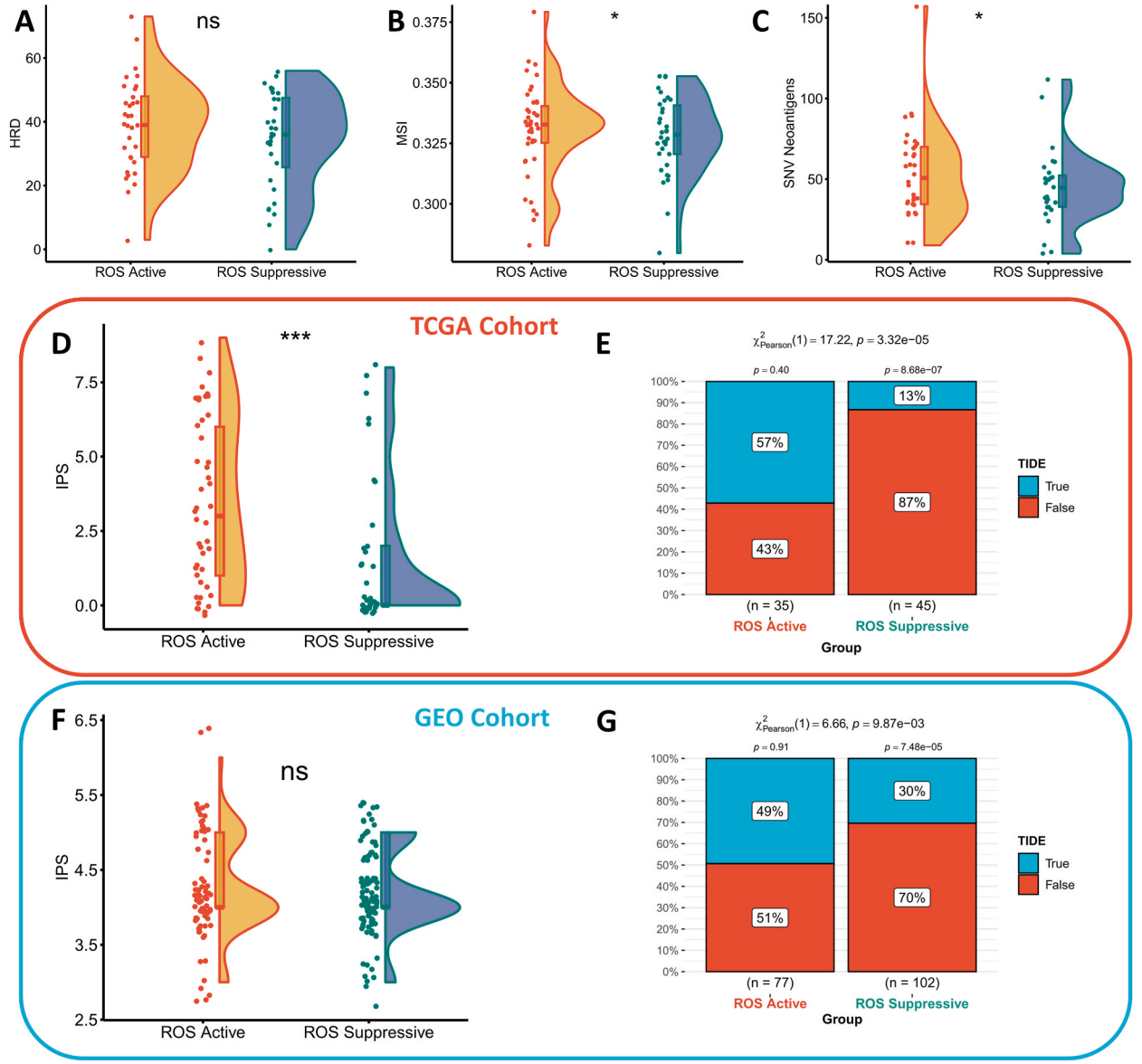


**Fig. 6.** Heterogeneity of immunotherapy response in different ROS subtypes (A) Violin plot demonstrating the difference in HRD between different ROS subtypes. (B) Violin plot demonstrating the differences in MSI among different ROS subtypes. (C) Violin plot demonstrating the differences in SNV neoantigens among different ROS subtypes. (D) Differences in IPS between different ROS subtypes in the TCGA-ESCC cohort and (F) GEO-ESCC cohort. TIDE algorithm predicts the response rates of patients with different ROS subtypes to immunotherapy in the (E) TCGA-ESCC cohort and (G) GEO-ESCC cohort. *: $P < 0.05$, ns: not significant.

immunotherapy (Fig. 6G).

### 3.7. Construction of a robust ROS activity score

To construct a robust ROS activity score, we first initially screened ROS-related DEGs with prognostic value by one-way Cox regression and survival log-rank test and obtained a total of 15 ROS-related DEGs after integration for further RAS generation. Subsequently, an iterative LASSO pipeline was used to generate a robust RAS model. After 1000 iterations and cross-validation, 14 variables were included with a penalty factor of 0.05182673 (Fig. 7A and B). Based on the LASSO coefficients and mRNA expression of these fourteen variables we generated the RAS, and the detailed gene coefficients have been uploaded as Table S2. Calculation of the C-index of RAS and other clinical variables suggested that RAS was a reliable predictor of OS for ESCC patients (Fig. 7C). Survival analysis showed that ESCC patients with high RAS had significantly shorter survival in both cohorts (Fig. 7D, Fig. S3A). ROC curves showed that RAS in the TCGA-ESCC cohort could effectively predict patient survival at 1, 2 and 3 years (AUC>0.80,Fig. 7E). In the GEO-ESCC cohort RAS could predict overall survival at 2 and 3 years (AUC>0.65, Fig. S3B). We also plotted tROC curves for RAS and patient clinical characteristics to assess the predictive efficacy of different variables over the disease cycle, and the results showed that RAS could be the best predictor of OS in both cohorts (Fig. 7F, Fig. S3C). Subsequently, univariate and multivariate Cox regression similarly confirmed that RAS was an independent and robust predictor of OS in both the TCGA-ESCC and GEO-ESCC cohorts (Fig. 7G and H). In addition, we analyzed the predictive efficacy of RAS in different clinical subgroups (Figs. S4A–B). Specifically, RAS could precisely predict the survival of ESCC patients in all age groups. However, RAS showed effective predictive ability only in male ESCC patients. In

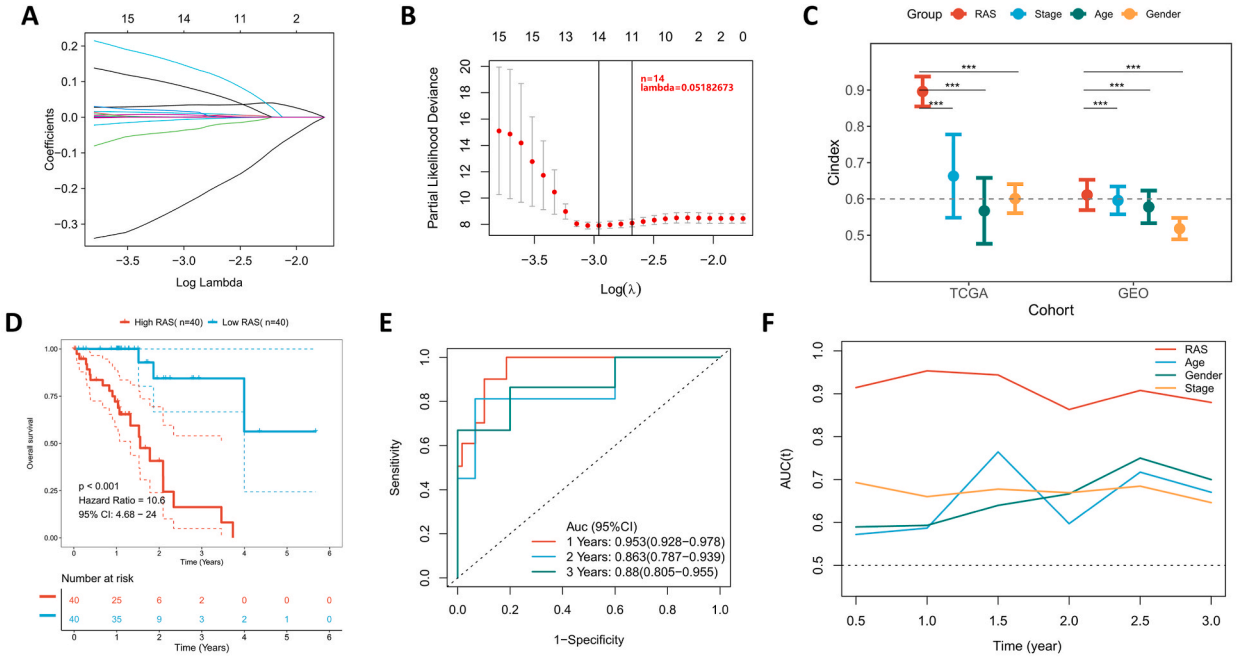


**G** Univariate Cox

| Variable | HR | lower 95%CI | upper 95%CI | pvalue |
|---|---|---|---|---|
| TCGA Cohort | | | | |
| Age | 1.022 | 0.977 | 1.069 | 3.43e−01 |
| Gender | 0.104 | 0.014 | 0.791 | 2.88e−02 |
| Stage | 2.030 | 1.208 | 3.411 | 7.50e−03 |
| RAS | 6.377 | 3.452 | 11.781 | 3.30e−09 |
| GEO Cohort | | | | |
| Age | 1.030 | 1.008 | 1.053 | 8.72e−03 |
| Gender | 1.278 | 0.799 | 2.045 | 3.07e−01 |
| Stage | 1.994 | 1.398 | 2.846 | 1.42e−04 |
| RAS | 5.673 | 2.490 | 12.925 | 3.60e−05 |

**H** Multivariate Cox

| Variable | HR | lower 95%CI | upper 95%CI | pvalue |
|---|---|---|---|---|
| TCGA Cohort | | | | |
| Age | 1.005 | 0.951 | 1.062 | 8.63e−01 |
| Gender | 0.213 | 0.019 | 2.367 | 2.08e−01 |
| Stage | 1.341 | 0.749 | 2.402 | 3.23e−01 |
| RAS | 5.807 | 3.107 | 10.853 | 3.54e−08 |
| GEO Cohort | | | | |
| Age | 1.026 | 1.002 | 1.050 | 3.01e−02 |
| Gender | 1.139 | 0.702 | 1.847 | 5.98e−01 |
| Stage | 1.969 | 1.369 | 2.830 | 2.55e−04 |
| RAS | 4.742 | 2.127 | 10.571 | 1.42e−04 |

**Fig. 7.** Generation of robust ROS active score (RAS) models (A–B) After iteration and cross-validation, the LASSO algorithm converged to a 14-gene RAS model based on the minimum lambda value (0.05182673). (C) Compared with other patient characteristics, RAS had the highest C-index. (D) KM survival curves for high and low RAS subgroups in the TCGA-ESCC cohort. (E) ROC analysis for the first three years of RAS in the TCGA-ESCC cohort. (F) tROC curves for the first three years of RAS in the TCGA-ESCC cohort. (G) Univariate regression analysis of OS in TCGA-ESCC and GEO-ESCC cohorts. (H) Multivariate regression analysis of OS in TCGA-ESCC and GEO-ESCC cohorts. ***: P < 0.001.

addition, RAS has more predictive power in patients with advanced ESCC, which is a meaningful addition to clinical application.

### 3.8. RAS can effectively predict immunotherapy

To assess the predictive efficacy of RAS for immunotherapy, we generated RAS in two real-world immunotherapy studies as previously mentioned. KM survival curves showed significantly lower overall survival in patients with high RAS than in patients with low RAS (Fig. 8A and B). We retrieved statistical patient neoantigens and TMB data from these two cohorts and assessed the correlation with RAS. The results showed that RAS had a significant negative correlation with neoantigens in the Imvigor210 cohort (Fig. 8C), while it did not show a significant correlation in the nature-SKCM cohort (Fig. 8D). Of interest, RAS showed a significant negative correlation with TMB in both immunotherapy cohorts (Fig. 8E and F).

### 3.9. RAS in a pan-cancer perspective

We assessed the genomic regulation as well as prognostic efficacy of RAS models in the TCGA-pancancer cohort. We first summarized the SNP frequencies of RAS model genes in 20 solid tumors. The results showed that RAS genes had high mutation frequency in non-small cell lung cancer, gastric cancer, and endometrial tumor, and VCAN, ATP10B, and NCAM2 were the three RAS genes with the highest mutation frequency (Fig. 9A). We then summarized all the mutated fragments and mapped the mutation profile of RAS genes in a pan-cancer perspective and the significant increase of RAS-associated mutations in endometriomas was able to be observed (Fig. 9B). We then examined the CNV events of RAS-related genes in the pan-cancer cohort and showed that KCND2, TWIST1, and HAS2 were the most frequently amplified genes, while C1QC, C1QA, and LDLRAD1 were the most frequently deletion genes (Fig. 9C). We then assessed the prognostic efficacy of RAS in the pan-cancer cohort by COX regression and Log-rank test. The results showed that RAS could be a reliable risk factor for esophageal, melanoma, and bladder cancers, which was consistent with the predictive effect in the immunotherapy cohort (Fig. 9D). Finally, we evaluated RAS-associated cancer pathway activity and summarized the GSEA enrichment results for 50 cancer-associated pathways in a pan-cancer cohort (Fig. 9E). Notably, P53 signaling pathway and TNF signaling pathway were positively associated with RAS levels in most solid tumors (Fig. 9E).

### 3.10. Preliminary validation of RAS model genes

Fig. 10A shows the risk coefficients of 14 RAS model genes, among which LDLRAD1 was the most powerful risk factor (coefficient

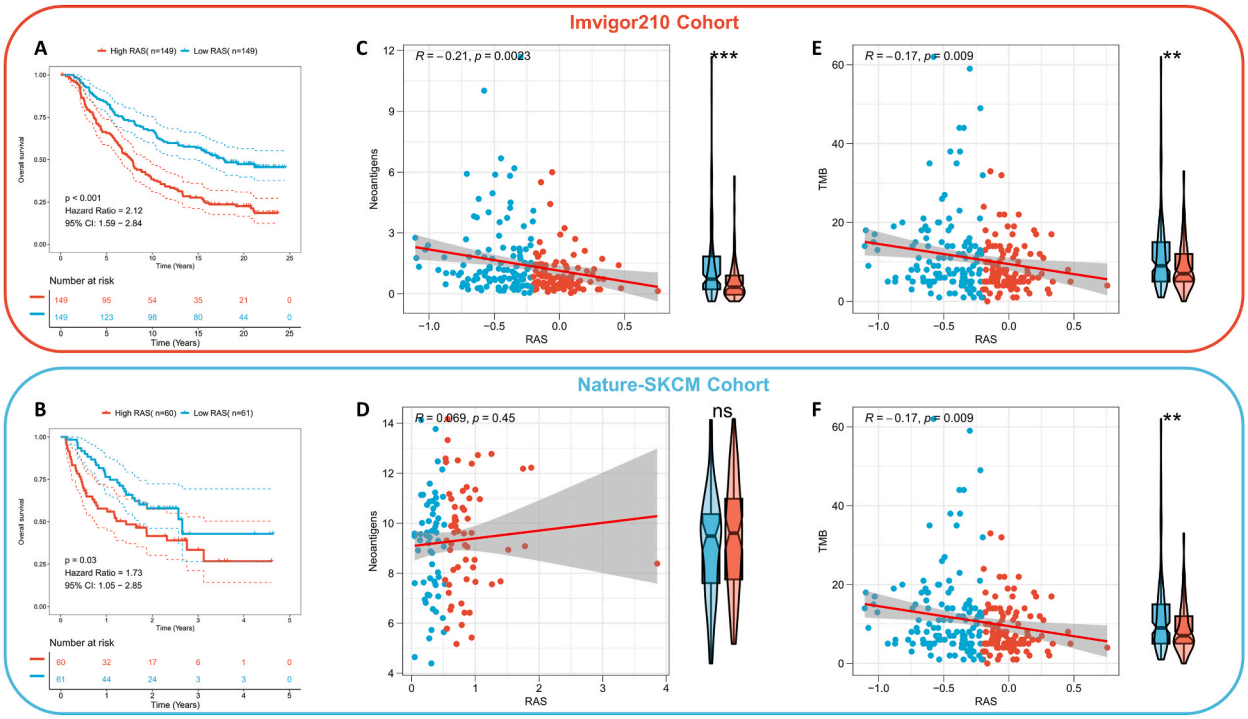


**Fig. 8.** Predictive efficacy of RAS in real-world immunotherapy cohorts (A) KM survival curves for the high RAS and low RAS subgroups in the Imvigor210 cohort. (B) KM survival curves of high RAS and low RAS subgroups in the Nature-SKCM cohort. (C) Correlation of RAS with Neoantigens in the Imvigor210 cohort. (D) Correlation of RAS with Neoantigens in the Nature-SKCM cohort. (E) Correlation between RAS and TMB in the Imvigor210 cohort. (F) Correlation of RAS with TMB in the Nature-SKCM cohort. **: $P < 0.01$, ***: $P < 0.001$, ns: not significant.

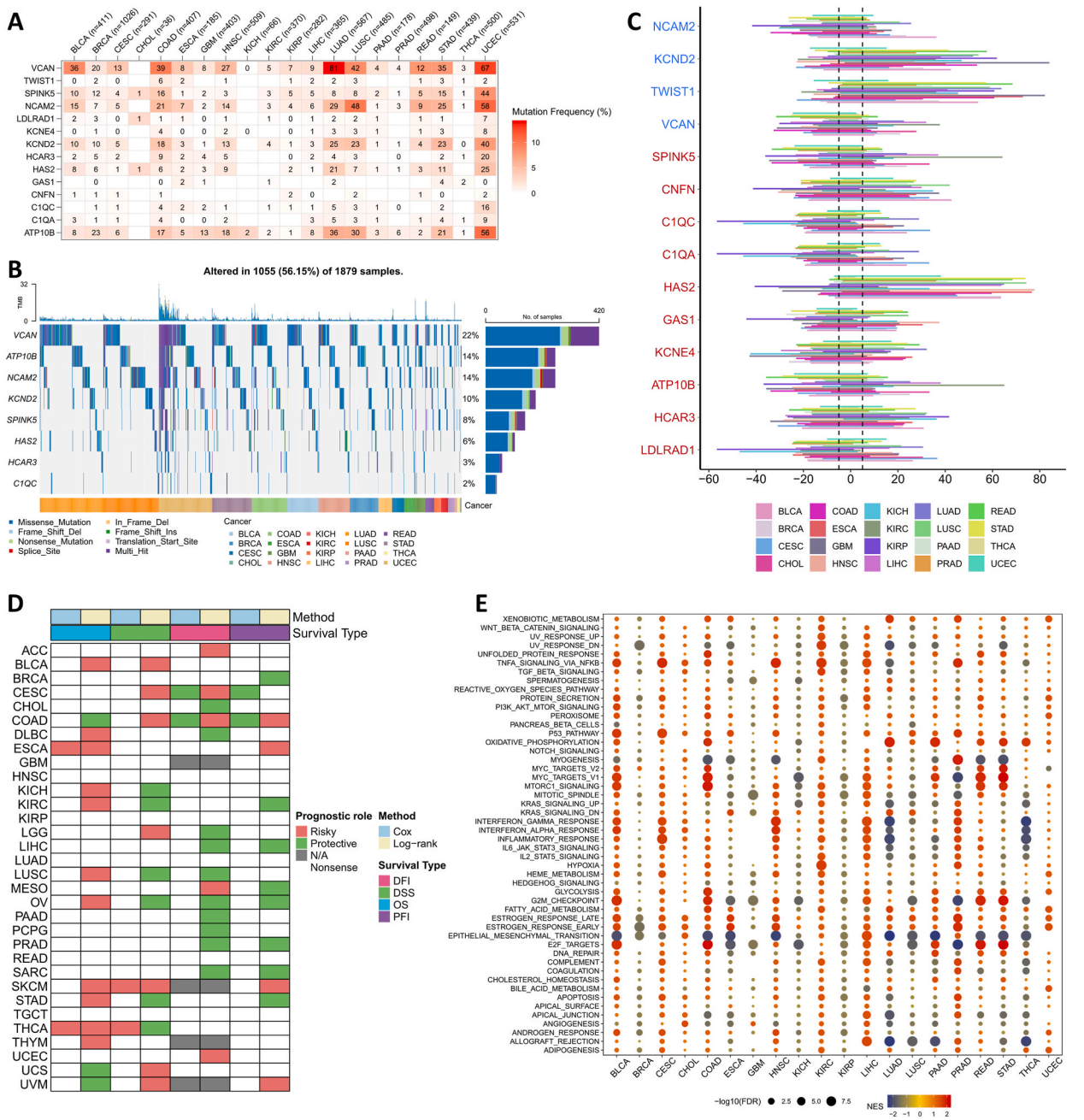


**Fig. 9.** Evaluation of RAS in a Pan-Cancer Perspective (A) summarized the mutation frequencies of RAS-related genes in 20 representative solid tumors. (B) After summarizing all mutation information, Oncoplot shows the mutation spectrum of RAS-related genes in the pan-cancer cohort. (C) CNV frequencies of RAS-associated genes in 20 representative solid tumors were summarized. (D) The predictive efficacy of RAS-associated genes for patient survival in 20 representative solid tumors was summarized. (E) Correlation of RAS features with cancer-related marker pathways (HALLMARK) in the pan-cancer cohort.

= 0.1421), so we tried to explore the regulation of LDLRAD1 for ESCC malignancy. We analyzed the prognostic efficacy of LDLRAD1 in the TCGA-pan cancer cohort and showed that LDLRAD1 could be used as a prognostic indicator for esophageal cancer, renal clear cell carcinoma, prostate cancer, and uterine sarcoma (Fig. 10B). Specifically, LDLRAD1 was an effective risk factor for OS in esophageal cancer, renal clear cell carcinoma, and prostate cancer, while it was a protective factor for OS in prostate cancer. We then examined the effect of LDLRAD1 on tumor cell proliferation activity in esophageal cancer cell lines using CCK-8. The results showed that the proliferative activity of both esophageal cancer cell lines (ECA-109 and TE1) silenced with LDLRAD1 was significantly stronger than that of the blank transfected group (Fig. 10C).

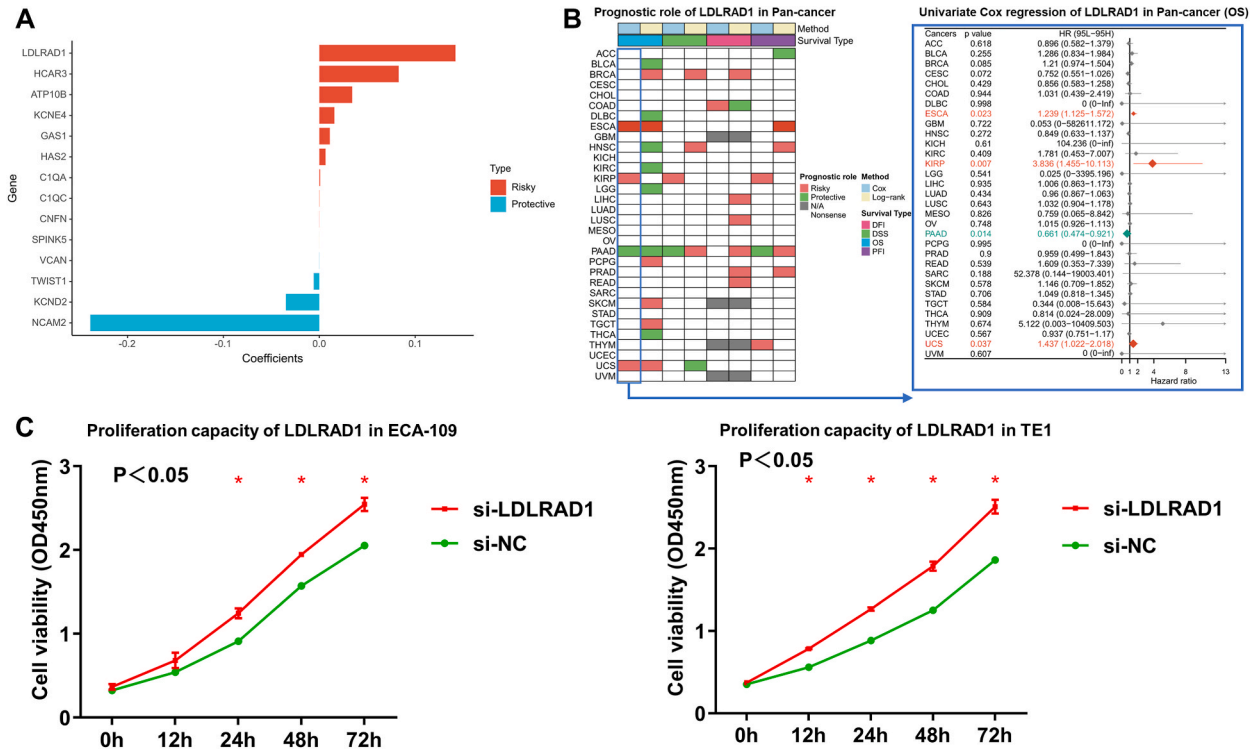


**Fig. 10.** Preliminary validation of the RAS core gene LDLRAD1 (A) Relative risk coefficients of RAS model genes. (B) Summary of the predictive efficacy of LDLRAD1 for patient survival in 20 representative solid tumors. (C) CCK-8 assay examined the effect of LDLRAD1 on cell proliferation activity in two esophageal cancer cell lines (left: ECA-109, right: TE1). *: P < 0.05.

## 4. Discussion

In recent years, esophageal cancer has progressed alarmingly worldwide and has gradually become a major type of cancer [30]. ESCC, the most common histopathological subtype of esophageal cancer, has a more aggressive degree of malignancy and leads to a worse prognosis [2]. The treatment of patients with advanced ESCC is a challenging problem, as conventional surgical resection is no longer feasible, and chemotherapy combined with novel therapies, including immunotherapy, becomes the last hope for ESCC patients [5]. ROS have complex and multiple roles in cancer, and recent studies have found that specific ROS levels can influence the immune system's response to cancer cells, thereby affecting the antitumor immune activity and the benefits of patients for immunotherapy [10,11]. However, the mechanisms by which ROS levels promote effective tumor treatment remain elusive. Our study focused on potentially heterogeneous ROS isoforms in ESCC and ultimately defined and validated two subtypes (ROS-active and ROS-suppressive) based on ROS-related pathway genes. The ROS-active subtype has stronger ROS activity, more potent cancer-associated immune pathway activity, and more infiltration of the effector immune cells. The ROS-suppressed subtype has weaker ROS activity but has more cell cycle dysregulation and a richer extracellular matrix, exhibiting characteristics of a malignant tumor. The reproducibility of the ROS-active and ROS-suppressive subtypes was confirmed in an external ESCC cohort from GEO. There was heterogeneity in the genomic stability of the two subtypes, particularly for CNV events. In addition, better outcomes in clinical outcomes and responses to immunotherapy existed for the ROS-active subtype. We constructed a RAS model to characterize ROS levels based on transcriptomic differences between the two ROS subtypes, and RAS can be used as a reliable predictor of OS in ESCC patients. Further analysis revealed the excellent efficacy of RAS in predicting patient outcomes in real-world immunotherapy cohorts. We also preliminarily validated the role of the core RAS gene (LDLRAD1) as a promoter of proliferation in esophageal cancer cell lines by CCK8 assays. These results provide a new perspective on transcriptomics for novel ROS-based clinical management and offer new directions for ROS-based immunotherapy.

Regarding the clinical characteristics of the two different ROS subtypes, we found that patients with the ROS-active phenotype had significantly better survival than the ROS-suppressive phenotype. Moreover, more patients with advanced ESCC stage were present in the ROS-suppressive phenotype, and it was more common for patients to experience disease progression. We analyzed the differences in biological functions among ROS subtypes in an attempt to reveal the potential regulatory mechanisms. Specifically, the functional enrichment results showed significant enrichment of immune signaling pathways (chemokines and cytokine receptors) [31,32], antigen presentation, and NK cell-mediated cell killing pathways mainly in the ROS active phenotype. In contrast, cell cycle-related pathways (e.g., Spliceosome and Peroxisome) [33,34], and cancer cell proliferation-related pathways (EGFR and P13K-AKT) were significantly enriched in the ROS-suppressed phenotype [35,36]. Subsequent exploration of the immune microenvironment revealed

more immune activity scores in the ROS-active phenotype, and significantly increased immune checkpoint expression and anti-tumor immune-related pathway activity. In addition, some effector immune cells, mainly NK cells and CD8 T cells, were also more infiltrated in the ROS-active phenotype [37,38]. Overall, the ROS-suppressed phenotype is an immune-silenced "cold" tumor environment, characterized by more extracellular matrix, less immune activity, and a lack of effector immune cells [39]. These findings suggest that the more effector immune cells and stronger immune activity in the ROS-active phenotype may have a stronger anti-tumor capacity, which may ultimately result in better survival and tumor remission rates in ESCC patients [40].

We then discussed the heterogeneity in genomic stability of the two ROS subtypes. TMB measured the overall SNP status of patients, however, we did not find significant TMB differences between the two ROS subtypes. Nevertheless, we noted a significantly higher frequency of mutations in the TRRAP gene in the ROS-active subtype. Previous studies have shown that TRRAP can be involved in cell cycle regulation to promote oncogenic transformation and promote tumor proliferation by activating mitotic genes. While mutations in TRRAP-encoding genes in ROS-active subtypes may cause phenotypic changes and lead to a better prognosis. CNV events provide insight into genomic stability in terms of chromosomal segments, and we found a significant increase in chromosomal amplification events in ROS-suppressed phenotypes, while deletion events were significantly upregulated on chromosome 10p, 17p, 18p and 18q arms. Relative to SNPs, CNV events play a dominant role in genomic stability differences between ROS subtypes. In conclusion, the genomic stability of different ROS subtypes was mainly regulated by CNV events. In addition, mutations in TRRAP may contribute to the differences in prognosis among patients with different ROS subtypes, suggesting that TRRAP may serve as a molecular target for novel clinical management and targeted therapy in ESCC patients.

We evaluated the potential benefits of immunotherapy in patients with different ROS subtypes in the TCGA-ESCC and GEO-ESCC cohorts. We detected a greater response to immunotherapy in patients with ROS-active subtypes. Therefore, we constructed a RAS score based on transcriptomic differences in ROS subtypes to assess patients' ROS levels and to precisely predict prognosis and immunotherapy. We confirmed in two ESCC cohorts that RAS could be a reliable risk factor for patient OS and performed more strongly in men and advanced ESCC patients. We generated RAS in a real-world immunotherapy study to assess the predictive efficacy of immunotherapy. The results showed that patients with high RAS had significantly worse survival than patients with low RAS. Neoantigens and TMB were reported predictors of immunotherapy and showed a high positive correlation with patients' response to immunotherapy [41,42]. We found that RAS was significantly negatively correlated with TMB in both immunotherapy cohorts and negatively correlated with neoantigens in the Imvigor210 cohort. This could partially explain the low response rate of patients with high RAS to immunotherapy. We also assessed the predictive efficacy of RAS in a pan-cancer perspective and surprisingly RAS was equally detrimental to OS in bladder cancer and melanoma, consistent with the cancer type of patients in the immunotherapy cohort. Finally, we demonstrated that knockdown of the core gene LDLRAD1 promotes the proliferation of esophageal cancer cells, which is inconsistent with our calculation results. We found heterogeneity in the effect of LDLRAD1 on patient prognosis among different cancer types in our pan-cancer analysis, and further experiments are needed to explore the specific mechanism of action.

Our study also has several shortcomings: a. We did not validate the reproducibility of ROS-related subtypes in more cohorts due to the lack of large-scale transcriptomic data in esophageal cancer; b. Genomic stability analysis from a single dataset is not convincing enough, and more whole-genome sequencing data are needed to assess the genomic heterogeneity of different ROS subtypes; c. The RAS model consists of more genes that are not convenient for clinical use, and more real-world clinical cohorts are needed to optimize the application of the RAS model in the future.

## 5. Conclusion

Our work identified heterogeneous ROS-active and ROS-suppressed subtypes in ESCC patients. The ROS-active subtype showed better clinical outcomes and response to immunotherapy. The ROS-active subtype had more active immune-related pathways and effector immune cell infiltration. The RAS signature developed based on ROS subtypes can effectively predict patient prognosis and immunotherapeutic benefit. These results provide a new perspective on transcriptomics for novel ROS-based clinical management and offer new directions for ROS-based immunotherapy.

## Data availability statement

The original contributions presented in the study are included in the article/supplementary material, further inquiries can be directed to the corresponding author.

## Funding

The study is supported by Key Program of Science and Technology Innovation Development Fund of Tangdu Hospital: 2019LCYJ004, "Elite Talents Cultivation Program - Top Talents" Project of Tangdu Hospital, Major clinical research project of Tangdu Hospital: 2021LCYJ008, Key Plan of New Technology and New Business in Tang Dou Hospital: XJSXYW2021001.

## CRediT authorship contribution statement

**Qiang Lu:** Writing – original draft, Visualization, Validation, Formal analysis, Data curation. **Qi Yang:** Writing – original draft, Software, Resources, Formal analysis, Data curation. **Jinbo Zhao:** Writing – review & editing, Writing – original draft, Validation, Data curation. **Guizhen Li:** Writing – review & editing, Writing – original draft, Funding acquisition, Data curation. **JiPeng Zhang:** Writing

– review & editing, Writing – original draft, Visualization, Validation, Software, Resources, Data curation. **Chenghui Jia:** Writing – review & editing, Resources, Data curation. **Yi Wan:** Writing – review & editing, Supervision, Project administration, Conceptualization. **Yan Chen:** Writing – review & editing, Supervision, Resources, Conceptualization.

## Declaration of competing interest

The authors declare that they have no known competing financial interests or personal relationships that could have appeared to influence the work reported in this paper.

## Acknowledgment

We sincerely thank the researchers for their dedication and the original data provided.

## Appendix A. Supplementary data

Supplementary data to this article can be found online at https://doi.org/10.1016/j.heliyon.2024.e35235.

## References

[1] H. Sung, J. Ferlay, R.L. Siegel, M. Laversanne, I. Soerjomataram, A. Jemal, et al., Global cancer statistics 2020: GLOBOCAN estimates of incidence and mortality worldwide for 36 cancers in 185 countries, CA A Cancer J. Clin. 71 (3) (2021) 209–249, https://doi.org/10.3322/caac.21660.
[2] Y. He, D. Liang, L. Du, T. Guo, Y. Liu, X. Sun, et al., Clinical characteristics and survival of 5283 esophageal cancer patients: a multicenter study from eighteen hospitals across six regions in China, Cancer Commun. 40 (10) (2020) 531–544, https://doi.org/10.1002/cac2.12087.
[3] C.C. Abnet, M. Arnold, W.Q. Wei, Epidemiology of esophageal squamous cell carcinoma, Gastroenterology 154 (2) (2018) 360–373, https://doi.org/10.1053/j.gastro.2017.08.023.
[4] Y.M. Yang, P. Hong, W.W. Xu, Q.Y. He, B. Li, Advances in targeted therapy for esophageal cancer, Signal Transduct. Targeted Ther. 5 (1) (2020) 229, https://doi.org/10.1038/s41392-020-00323-3.
[5] J.E. Rogers, M. Sewastjanow-Silva, R.E. Waters, J.A. Ajani, Esophageal cancer: emerging therapeutics, Expert Opin. Ther. Targets 26 (2) (2022) 107–117, https://doi.org/10.1080/14728222.2022.2036718.
[6] P. Gotwals, S. Cameron, D. Cipolletta, V. Cremasco, A. Crystal, B. Hewes, et al., Prospects for combining targeted and conventional cancer therapy with immunotherapy, Nat. Rev. Cancer 17 (5) (2017) 286–301, https://doi.org/10.1038/nrc.2017.17.
[7] D. Uprety, S.J. Mandrekar, D. Wigle, A.C. Roden, A.A. Adjei, Neoadjuvant immunotherapy for NSCLC: current concepts and future approaches, J. Thorac. Oncol. : official publication of the International Association for the Study of Lung Cancer 15 (8) (2020) 1281–1297, https://doi.org/10.1016/j.jtho.2020.05.020.
[8] U.S. Srinivas, B.W.Q. Tan, B.A. Vellayappan, A.D. Jeyasekharan, ROS and the DNA damage response in cancer, Redox Biol. 25 (2019) 101084, https://doi.org/10.1016/j.redox.2018.101084.
[9] Q. Cui, J.Q. Wang, Y.G. Assaraf, L. Ren, P. Gupta, L. Wei, et al., Modulating ROS to overcome multidrug resistance in cancer, Drug Resist. Updates : reviews and commentaries in antimicrobial and anticancer chemotherapy 41 (2018) 1–25, https://doi.org/10.1016/j.drup.2018.11.001.
[10] C.L. Kuo, A. Ponneri Babuharisankar, Y.C. Lin, H.W. Lien, Y.K. Lo, H.Y. Chou, et al., Mitochondrial oxidative stress in the tumor microenvironment and cancer immunoescape: foe or friend? J. Biomed. Sci. 29 (1) (2022) 74, https://doi.org/10.1186/s12929-022-00859-2.
[11] R. Liu, L. Peng, L. Zhou, Z. Huang, C. Zhou, C. Huang, Oxidative stress in cancer immunotherapy: molecular mechanisms and potential applications, Antioxidants 11 (5) (2022), https://doi.org/10.3390/antiox11050853.
[12] L. Bracci, G. Schiavoni, A. Sistigu, F. Belardelli, Immune-based mechanisms of cytotoxic chemotherapy: implications for the design of novel and rationale-based combined treatments against cancer, Cell Death Differ. 21 (1) (2014) 15–25, https://doi.org/10.1038/cdd.2013.67.
[13] E.L. Yarosz, C.H. Chang, The role of reactive oxygen species in regulating T cell-mediated immunity and disease, Immune network 18 (1) (2018) e14, https://doi.org/10.4110/in.2018.18.e14.
[14] K.B. Kennel, F.R. Greten, Immune cell - produced ROS and their impact on tumor growth and metastasis, Redox Biol. 42 (2021) 101891, https://doi.org/10.1016/j.redox.2021.101891.
[15] D. Mougiakakos, C.C. Johansson, R. Kiessling, Naturally occurring regulatory T cells show reduced sensitivity toward oxidative stress-induced cell death, Blood 113 (15) (2009) 3542–3545, https://doi.org/10.1182/blood-2008-09-181040.
[16] A. Liberzon, A. Subramanian, R. Pinchback, H. Thorvaldsdóttir, P. Tamayo, J.P. Mesirov, Molecular signatures database (MSigDB) 3.0, Bioinformatics 27 (12) (2011) 1739–1740, https://doi.org/10.1093/bioinformatics/btr260.
[17] G. Yu, L.G. Wang, Y. Han, Q.Y. He, clusterProfiler: an R package for comparing biological themes among gene clusters, OMICS A J. Integr. Biol. 16 (5) (2012) 284–287, https://doi.org/10.1089/omi.2011.0118.
[18] K. Yoshihara, M. Shahmoradgoli, E. Martínez, R. Vegesna, H. Kim, W. Torres-Garcia, et al., Inferring tumour purity and stromal and immune cell admixture from expression data, Nat. Commun. 4 (2013) 2612, https://doi.org/10.1038/ncomms3612.
[19] A.M. Newman, C.L. Liu, M.R. Green, A.J. Gentles, W. Feng, Y. Xu, et al., Robust enumeration of cell subsets from tissue expression profiles, Nat. Methods 12 (5) (2015) 453–457, https://doi.org/10.1038/nmeth.3337.
[20] V. Thorsson, D.L. Gibbs, S.D. Brown, D. Wolf, D.S. Bortone, T.H. Ou Yang, et al., The immune landscape of cancer, Immunity 48 (4) (2018) 812–830, https://doi.org/10.1016/j.immuni.2018.03.023.
[21] A. Mayakonda, D.C. Lin, Y. Assenov, C. Plass, H.P. Koeffler, Maftools: efficient and comprehensive analysis of somatic variants in cancer, Genome Res. 28 (11) (2018) 1747–1756, https://doi.org/10.1101/gr.239244.118.
[22] P. Blanche, C. Proust-Lima, L. Loubère, C. Berr, J.F. Dartigues, H. Jacqmin-Gadda, Quantifying and comparing dynamic predictive accuracy of joint models for longitudinal marker and time-to-event in presence of censoring and competing risks, Biometrics 71 (1) (2015) 102–113, https://doi.org/10.1111/biom.12232.
[23] P. Charoentong, F. Finotello, M. Angelova, C. Mayer, M. Efremova, D. Rieder, et al., Pan-cancer immunogenomic analyses reveal genotype-immunophenotype relationships and predictors of response to checkpoint blockade, Cell Rep. 18 (1) (2017) 248–262, https://doi.org/10.1016/j.celrep.2016.12.019.
[24] P. Jiang, S. Gu, D. Pan, J. Fu, A. Sahu, X. Hu, et al., Signatures of T cell dysfunction and exclusion predict cancer immunotherapy response, Nat. Med. 24 (10) (2018) 1550–1558, https://doi.org/10.1038/s41591-018-0136-1.
[25] J. Fu, K. Li, W. Zhang, C. Wan, J. Zhang, P. Jiang, et al., Large-scale public data reuse to model immunotherapy response and resistance, Genome Med. 12 (1) (2020) 21, https://doi.org/10.1186/s13073-020-0721-z.
[26] C. Wang, X. Gu, X. Zhang, M. Zhou, Y. Chen, Development and validation of an E2F-related gene signature to predict prognosis of patients with lung squamous cell carcinoma, Front. Oncol. 11 (2021) 756096, https://doi.org/10.3389/fonc.2021.756096.

[27] Y. Wang, H. Tan, T. Yu, X. Chen, F. Jing, H. Shi, Potential immune biomarker candidates and immune subtypes of lung adenocarcinoma for developing mRNA vaccines, Front. Immunol. 12 (2021) 755401, https://doi.org/10.3389/fimmu.2021.755401.
[28] A. Necchi, R.W. Joseph, Y. Loriot, J. Hoffman-Censits, J.L. Perez-Gracia, D.P. Petrylak, et al., Atezolizumab in Platinum-Treated Locally Advanced or Metastatic Urothelial Carcinoma: Post-progression Outcomes from the Phase II IMvigor210 Study, 2010, pp. 1569–8041.
[29] D. Liu, B.A.-O. Schilling, D. Liu, A. Sucker, E. Livingstone, L. Jerby-Arnon, et al., Integrative Molecular and Clinical Modeling of Clinical Outcomes to PD1 Blockade in Patients with Metastatic Melanoma, 2020, pp. 1546–1570.
[30] J.K. Waters, S.I. Reznik, Update on management of squamous cell esophageal cancer, Curr. Oncol. Rep. 24 (3) (2022) 375–385, https://doi.org/10.1007/s11912-021-01153-4.
[31] A.J. Ozga, M.T. Chow, A.D. Luster, Chemokines and the immune response to cancer, Immunity 54 (5) (2021) 859–874, https://doi.org/10.1016/j.immuni.2021.01.012.
[32] W.C. Chou, E. Rampanelli, X. Li, J.P. Ting, Impact of intracellular innate immune receptors on immunometabolism, Cell. Mol. Immunol. 19 (3) (2022) 337–351, https://doi.org/10.1038/s41423-021-00780-y.
[33] Z. Karamysheva, L.A. Díaz-Martínez, R. Warrington, H. Yu, Graded requirement for the spliceosome in cell cycle progression, Cell Cycle 14 (12) (2015) 1873–1883, https://doi.org/10.1080/15384101.2015.1039209.
[34] S. Theocharis, A. Margeli, P. Vielh, G. Kouraklis, Peroxisome proliferator-activated receptor-gamma ligands as cell-cycle modulators, Cancer Treat Rev. 30 (6) (2004) 545–554, https://doi.org/10.1016/j.ctrv.2004.04.004.
[35] B.R. Voldborg, L. Damstrup, M. Spang-Thomsen, H.S. Poulsen, Epidermal growth factor receptor (EGFR) and EGFR mutations, function and possible role in clinical trials, Ann. Oncol. : official journal of the European Society for Medical Oncology 8 (12) (1997) 1197–1206, https://doi.org/10.1023/a:1008209720526.
[36] J.S. Yu, W. Cui, Proliferation, survival and metabolism: the role of PI3K/AKT/mTOR signalling in pluripotency and cell fate determination, Development (Cambridge, England) 143 (17) (2016) 3050–3060, https://doi.org/10.1242/dev.137075.
[37] M. St Paul, P.S. Ohashi, The roles of CD8(+) T cell subsets in antitumor immunity, Trends Cell Biol. 30 (9) (2020) 695–704, https://doi.org/10.1016/j.tcb.2020.06.003.
[38] S. Liu, V. Galat, Y. Galat, Y.K.A. Lee, D. Wainwright, J. Wu, NK cell-based cancer immunotherapy: from basic biology to clinical development, J. Hematol. Oncol. 14 (1) (2021) 7, https://doi.org/10.1186/s13045-020-01014-w.
[39] P. Bonaventura, T. Shekarian, V. Alcazer, J. Valladeau-Guilemond, S. Valsesia-Wittmann, S. Amigorena, et al., Cold tumors: a therapeutic challenge for immunotherapy, Front. Immunol. 10 (2019) 168, https://doi.org/10.3389/fimmu.2019.00168.
[40] M.Z. Madden, J.C. Rathmell, The complex integration of T-cell metabolism and immunotherapy, Cancer Discov. 11 (7) (2021) 1636–1643, https://doi.org/10.1158/2159-8290.Cd-20-0569.
[41] T.N. Schumacher, R.D. Schreiber, Neoantigens in cancer immunotherapy, Science (New York, NY) 348 (6230) (2015) 69–74, https://doi.org/10.1126/science.aaa4971.
[42] R. Cristescu, R. Mogg, M. Ayers, A. Albright, E. Murphy, J. Yearley, et al., Pan-tumor genomic biomarkers for PD-1 checkpoint blockade-based immunotherapy, Science (New York, NY) 362 (6411) (2018), https://doi.org/10.1126/science.aar3593.